



Oscillations and Waves in Radio Source of Drifting Pulsation Structures

Marian Karlický¹  · Ján Rybák²  ·
Miroslav Bárta¹

© Springer

Abstract Drifting pulsation structures (DPSs) are considered to be radio signatures of the plasmoids formed during magnetic reconnection in the impulsive phase of solar flares. In the present paper we analyze oscillations and waves in seven examples of drifting pulsation structures, observed by the 800–2000 MHz Ondřejov radiospectrograph. For their analysis we use a new type of oscillation maps which give us a much more information about processes in DPSs than that in previous analyzes. Based on these oscillation maps, made from radio spectra by the wavelet technique, we recognized quasi-periodic oscillations with periods ranging from about 1 to 108 s in all studied DPSs. This strongly supports the idea that DPSs are generated during a fragmented magnetic reconnection. Phases of most the oscillations in DPSs, especially for the period around 1 s, are synchronized (“infinite” frequency drift) in the whole frequency range of DPSs. For longer periods in some DPSs we found that the phases of the oscillations drift with the frequency drift in the interval from -17 to $+287 \text{ MHz s}^{-1}$. We propose that these drifting phases can be caused (a) by the fast or slow magnetosonic waves generated during the magnetic reconnection and propagating through the plasmoid, (b) by a quasi-periodic structure in the plasma inflowing to the reconnection forming a plasmoid, and (c) by a quasi-periodically varying reconnection rate in the X-point of the reconnection close to the plasmoid.

Keywords: Sun: flares – Sun: radio radiation – Sun: oscillations

✉ J. Rybák
rybak@astro.sk

¹ Astronomical Institute, Academy of Sciences of the Czech Republic, 251 65 Ondřejov, Czech Republic

² Astronomical Institute, Slovak Academy of Sciences, Tatranská Lomnica, Slovakia

1. Introduction

Drifting pulsation structure was for the first time recognized in the paper by Kliem, Karlický, and Benz (2000). It was interpreted as radio emission from the plasmoid formed during magnetic reconnection in the impulsive phase of solar flares. Details of this interpretation were presented in the papers by Karlický and Bárta (2007); Bárta, Vršnak, and Karlický (2008); Bárta, Karlický, and Žemlička (2008); Karlický, Bárta, and Rybák (2010); Bárta *et al.* (2011); Karlický and Bárta (2011) and can be summarized as follows. In the flare current sheet, formed below the rising magnetic rope during magnetic reconnection, plasmoids are generated due to the tearing-mode/plasmoid instability (Loureiro, Schekochihin, and Cowley, 2007). At the X-points of the magnetic reconnection, superthermal electrons are accelerated (Karlický, 2008). Then these electrons are trapped in a nearby plasmoid, where they generate plasma waves. These waves are then converted to the electromagnetic waves observed as DPSs (Karlický, Bárta, and Rybák, 2010). The narrow bandwidth of DPSs is caused by the limited interval of the plasma densities (plasma frequencies) inside the plasmoid. Due to divergence of the magnetic field lines in the upward direction in the solar atmosphere plasmoids preferentially move upwards (Bárta, Vršnak, and Karlický, 2008), that is why DPSs mostly drift toward low frequencies. The velocity of plasmoids can be as high as the local Alfvén speed. The acceleration of electrons at X-points of magnetic reconnection is believed to be quasi-periodic, which causes quasi-periodic pulsations of DPSs.

As mentioned above, the plasmoid is an important part of the magnetic reconnection process. Thus, the corresponding DPSs can be used for diagnostics of processes in magnetic reconnection in solar flares. Some analysis of DPSs were made in the papers by Karlický *et al.* (2005); Dabrowski, Karlický, and Rudawy (2015). For example, DPS observed during the 12 April 2001 flare with the high time resolution (1 ms) on the single frequencies of 610 and 1420 MHz was analyzed by the Fourier method and periods in the interval of 0.9–7.5 s were found (Karlický *et al.*, 2005). For an interval of periods shorter than 1 s the authors found that the periods are distributed according to the power-law function with the power-law index from -1.3 to -1.6 . The power-law distribution with the similar power-law index was also found in the 0.025–0.1 s period interval in DPS from the 12 July 2000 flare, observed with the very high time resolution ($80 \mu\text{s}$) by the 1352–1490 MHz *Torun Radiospectrograph* (Dabrowski, Karlický, and Rudawy, 2015).

In the present paper, we continue in the analysis of DPSs and thus processes in the radio source of DPSs, *i.e.*, processes in plasmoids. But, compared with the previous studies we use a much more sophisticated method, which was for the first time used in the paper by Karlický and Rybák (2017). This new method gives us a more detailed information about waves and oscillations in DPSs. We analyze a set of DPSs in order to obtain some statistics about these processes.

The paper is organized as follows: In Section 2 we show data and describe methods of their analysis. The results of the analysis are summarized in Section 3. In Section 4 the results are interpreted and conclusions are summarized in Section 5.

Table 1. List of the studied DPSs and the parameters of the soft X-ray emission of the related solar flares.

DPS no.	Date	Flare start (UT)	Flare maximum (UT)	Flare end (UT)	GOES classification
1	1992 Oct. 5	09:13	09:31	09:56	M2.0
2	1998 Aug. 18	08:14	08:24	08:32	X2.8
3	2002 May 20	15:21	15:27	15:31	X2.1
4	2002 Aug. 30	12:47	13:29	13:35	X1.5
5	2003 May 27	05:06	06:26	07:16	M1.6
6	2005 Jun. 14	06:54	07:30	07:56	C4.2
7	2014 Apr. 18	12:31	13:03	13:20	M7.3

2. Data and Methods of Their Analysis

The radio spectra of seven DPSs selected for our analysis, listed in Table 1, were acquired by *Ondřejov Radiospectrograph* RT5 located at Ondřejov, Czech Republic. Radiospectrograph frequency range, frequency resolution, and temporal resolution of the instrument are 800–2000 MHz, 4.7 MHz, and 10 ms, respectively (Jiříčka and Karlický, 2008). No special data reduction has been applied to the archive data of the RT5 radiospectrograph. Data were only re-sampled to the final temporal sampling of 0.1 s (1 s for DPS No.7). At some frequencies, man-made radio interference affected the acquired signal. Such parts of the data are excluded and they are marked by black bands in all plots of the radiospectrograms. Plots of three radiospectrograms can be seen as the second panels in Figures 1 (DPS No.1), 3 (DPS No.3), and 5 (DPS No.7).

For analysis of the radio spectra we utilize a novel method introduced in articles of Karlický and Rybák (2017) and Karlický, Rybák, and Monstein (2017). This method is based on the wavelet transform (WT) (Torrence and Compo, 1998) providing a clear detection of time–frequency evolution of the strong radio signal wave-patterns. The statistically significant wave-pattern signal power is identified in the selected period range at any temporal moment and radio frequency. Then the method provides an overplot of the phases of the detected significant radio signal wave-patterns at their temporal and frequency locations on a plot of the original radiospectrogram. Due to possible multiplicity of the signal periodicities the investigated periodicities have to be limited to narrower WT period ranges of particular interest.

In this work the Morlet mother wavelet, consisting of a complex sine wave modulated by a Gaussian, is selected to search for radio signal variability, with the non-dimensional frequency ω_0 satisfying the admissibility condition (Farge, 1992). The WT is calculated for the period range from 0.1 to 20 s (1 to 200 s for DPS No.7) with scales sampled as fractional powers of two with $\delta j = 0.4$, which is small enough to give an adequate sampling in scale, a minimum scale $s_j = 0.096$ s (0.96 s for DPS No.7) and a number of scales $N = 101$. Both the calculated significance of the derived WT periodicities and the cone-of-influence

Table 2. Radio emission parameters of studied DPSs.

DPS no.	Date	Time (UT)	Frequency range [GHz]	Frequency drift [MHz s ⁻¹]
1	1992 Oct. 5	09:24:20–09:25:00	1.0–1.7	–12.1
2	1998 Aug. 18	08:18:20–08:18:40	0.8–1.4	–7.1
3	2002 May 20	15:24:55–15:25:28	1.0–1.7	–25.0
4	2002 Aug. 30	13:27:38–13:27:50	0.8–1.5	–30.0
5	2003 May 27	06:42:36–06:43:28	0.8–1.3	–6.3
6	2005 Jun. 14	07:21:32–07:22:20	1.0–1.5	–5.5
7	2014 Apr. 18	12:44:00–12:53:00	0.8–1.6	–1.66

are taken into account as described in Karlický and Rybák (2017). The value of the confidence level was set to 99 %.

3. Results

We analyzed the DPSs observed in seven solar flares, which parameters are shown in Tables 1 and 2. From the comparison of Table 1 and Table 2 it can be seen, except the 27 May 2003 event (DPS No.5), that the DPSs were observed before the GOES soft X-ray flare maximum.

An overall inspection of the radio spectra shows that all these DPSs drift towards low frequencies with the frequency drift in the range from -1.66 to -30 MHz s^{-1} (Table 2).

Using the method described in the previous section we constructed for all DPSs oscillation maps of the phases for intervals around all detected statistically significant main oscillation periods. These main oscillation periods are listed in Table 3 (second column).

Examples of the DPS radio spectra together with the corresponding phase oscillation maps are shown in Figures 1 and 2 (DPS No.1), 3 and 4 (DPS No.3), and 5 and 6 (DPS No.7).

These figures start with the histogram of the WT significant periods detected in the DPS at the top of the first figure. Peaks in these histograms represent the main periods of oscillations found in the DPS which are numerically listed in the second column of Table 3. They were found for periods in the 1–108 s range. Around these peaks we selected the ranges of periods for computation of the oscillation maps (see below the discussion on how this period-range selection influences the results). The next plot (from up to down) shown in the figure is the DPS radiospectrum itself. The phase oscillation maps, showing phase of the statistically significant oscillations (pink areas with the black lines showing the zero phase) are shown then in consecutive plots in these couples of figures starting from maps for the short periods to those for longer periods.

Table 3. Main oscillation periods and parameters of the most distinct drifting phases (DPHA) of oscillations found in DPSs. The DPHAs are marked by the white arrows in Figures 2, 4 and 6.

DPS No.	Main oscillation periods [s]	DPHA time (UT)	DPHA frequency [GHz]	DPHA freq. drift [MHz s ⁻¹]	DPHA period [s]
1	0.9–1.7, 2.4,	9:24:27.2–9:24:28.0	1.47–1.7	+287	6.5–8.5
	3.9, 4.8, 5.2, 7.8, 9.2	9:24:43.5–9:24:44.7	1.1–1.25	+125	6.5–8.5
2	0.5–1.3, 2.0, 3.0, 3.5, 6.9, 9.1, 13.3	no DPHA			
3	1.0–1.6, 2.2, 2.9, 3.2, 4.9 5.7, 8.9	15:25:11.2–15:25:12.4	1.35–1.5	–125	7.2–10.5
4	0.7, 1.0, 2.0, 3.0	no DPHA			
5	0.5–1.5, 1.7, 2.8, 3.8–5.6, 8.5	no DPHA			
6	0.5–1.0, 1.1, 2.1, 3.0, 4.1, 5.9	no DPHA			
7	18, 30, 65,	12:46:30–12:46:48	1.2–1.5	–17	65–115
	90, 108	12:49:18–12:49:36	1.1–1.47	–21	63–75

In all DPSs, we found that at short periods the phases are more or less synchronized; they have an "infinite" frequency drift. On the other hand, for three DPSs (Nos. 1, 3 and 7) and for longer periods, the phases of some oscillations drift in frequencies. In Figures 1–6 the most distinct drifting phases are designated by white arrows and their parameters are summarized in Table 3. Drifts of these oscillation phases (DPHA) were found to be in the range from -17 to $+287 \text{ MHz s}^{-1}$.

To show how these oscillation maps depend on the selected interval of periods, in Figure 6 we present not only the phase maps for distinct period intervals of the 63–75 and 78–95 s (third and fourth panels), but also the map for the 65–115 s period (the bottom panel), which covers both these 63–75 and 78–95 s period ranges. Comparing these maps we can see how phases presented in the map with a broader range of periods are distributed in the time–frequency domain in the maps with narrower ranges of periods.

Furthermore, comparing the parameters of DPSs (Table 2) with those of oscillation periods and drifting phases DPHA we can see that the DPS No. 7 (18 April 2014) differs from other DPSs. This DPS has not only the smallest frequency drift (-1.66 MHz s^{-1}), but also much longer main periods (up to 108 s) as well

as smaller absolute frequency drift of drifting phases (-17 and -21 MHz s^{-1}) comparing to other DPSs. In other DPSs the interval of oscillation periods is up to 15 s, approximately.

4. Interpretation

In this work we are interested not only about periods of oscillations in DPSs, but also about the frequency drifts of phases of these oscillations. Namely, DPSs are generated by the plasma emission mechanism (Bárta, Karlický, and Žemlička, 2008), therefore the emission frequency is connected with the plasma density and thus with the altitude of the radio source in the gravitationally stratified solar atmosphere. Therefore, the very high frequency drift of oscillation phases can be interpreted by the high speed of the superthermal electrons injected into the plasmoid. On the other hand, their low frequency drift can indicate a presence of some magnetohydrodynamic waves or plasma density structures in or close to the plasmoid.

Analyzing seven DPSs by a new type of oscillation maps, we found oscillations with periods in the range 0.5–13.3 s for six DPSs (Nos. 1–6) and in the range 7–108 s for DPS No. 7. The frequency drift of the DPSs No. 1–6 (from -5.5 to -30 MHz s^{-1}) was greater than that of the DPS No. 7 (-1.66 MHz s^{-1}).

We found that oscillations especially for short periods are practically synchronized ("infinite" frequency drift). This synchronization with the period of about 1 s confirms findings in our previous studies (Kliem, Karlický, and Benz, 2000; Karlický, 2014) and shows that the used wavelet method works correctly. In agreement with our previous papers we interpret this synchronization as caused by a quasi-periodic injection of fast superthermal electrons into the plasmoid. A broad range of periods of the oscillations with "infinite" drift is a new result and we think that it is caused by fragmented magnetic reconnection, where particles are accelerated during the merging of plasmoids of different sizes and thus with different periods (Karlický and Bárta, 2011; Bárta *et al.*, 2011).

In DPSs No. 1, 3 and 7 for longer oscillation periods we found the oscillations with drifting phases. In DPS No. 1 the frequency drift of drifting phase (oscillation period 6.5–8.5 s) was positive ($+287$ and $+125 \text{ MHz s}^{-1}$), in DPS No. 3 (oscillation period 7.2–10.5 s) negative (-125 MHz s^{-1}), and in DPS No. 7 (oscillation period 65–115 s) negative (-17 and -21 MHz s^{-1}), but its absolute value was much smaller than in the DPSs No. 1 and 3.

As shown in the papers by Bárta *et al.* (2007) and Jelínek *et al.* (2017) magnetic reconnection is closely connected with magnetosonic waves, which are generated at regions of enhanced (anomalous) resistivity appear. At these regions the plasma is strongly heated, its pressure increases and thus the magnetosonic waves are generated and propagate out of these regions. Generally, there are many such regions around X-points of the fragmented magnetic reconnection, therefore it is highly probable that some of these will interact with the plasmoid producing the DPS. Such waves can modulate the plasma density and thus modulate a DPS emission, as described *e.g.* in the papers by Karlický, Mészárosová, and Jelínek (2013) and Karlický (2013).

Based on these results, the frequency drift of the drifting oscillation phase can be interpreted as caused by magnetosonic waves in (or in close vicinity of) the plasmoid. If we take the size of the plasmoid (where DPS is generated) as in the papers by Ohyama and Shibata (1998); Karlický and Kliem (2010) (10 or 25 Mm) and the Alfvén speed at the plasmoid as 1000 km s^{-1} , approximately, then the drifting oscillation phases in DPSs No. 1 and 3 can be caused by the fast magnetosonic wave. Their positive and negative frequency drifts are then caused by the waves propagating through the plasmoid in the direction of the density gradient or in the opposite direction.

Period of drifting oscillation phases in DPS No. 7 are too long to be interpreted as in the case of DPSs No. 1 and 3. We propose that in this DPS No. 7 the drifting oscillation phases are caused by the slow magnetosonic waves.

Besides interpretation of the drifting phases by the magnetosonic waves, there are also other possible interpretations, *e.g.* by a quasi-periodic structure in the plasma inflowing to the reconnection forming the plasmoid and by a quasi-periodically varying reconnection rate in the X-point of the reconnection close to the plasmoid. We think that both these processes generate the quasi-periodic density structure of the plasmoid and this structure, as the plasmoid grows, can modulate the DPS.

5. Conclusions

This study gives us new and more detailed information about oscillations and waves in and around the plasmoid formed during the flare magnetic reconnection.

We analyzed seven DPSs observed by the *Ondřejov Radiospectrograph*. Using a new type of oscillation maps, we found that DPSs are very rich in oscillations in the range of 1–108 s periods. This strongly supports the idea that DPSs are generated in the plasmoid during fragmented magnetic reconnection.

In all DPSs, especially for shorter periods, the oscillations were synchronized in the whole range of DPSs. In agreement with a theoretical interpretation of the DPSs, we propose that these synchronized oscillations are caused by quasi-periodic injections of the superthermal electrons into the plasmoid from fragmented magnetic reconnection.

On the other hand, in some DPSs and mostly for longer periods we found oscillations having their phases drifting in frequencies. In assumed plasma emission mechanism of DPSs it indicates a presence of some magnetosonic waves in and around the plasmoid or some evolving density structure in the plasmoid. We propose that the oscillations with drifting phases can be caused (a) by fast or slow magnetosonic waves, generated during fragmented magnetic reconnection and propagating through the plasmoid, (b) by a quasi-periodic structure in the plasma inflowing to the reconnection region forming the plasmoid, and (c) by a quasi-periodically varying reconnection rate in the X-point of reconnection close to the plasmoid.

Acknowledgments This research was supported by Grants 16-13277S and 17-16447S of the Grant Agency of the Czech Republic. This work was supported by the Science Grant Agency

project VEGA 2/0004/16 (Slovakia). Help of the Bilateral Mobility Projects SAV-16-03 and SAV-18-01 of the SAS and CAS is acknowledged. This article was created in the project ITMS No. 26220120029, based on the supporting operational Research and development program financed from the European Regional Development Fund. This research has made use of NASA's Astrophysics Data System. The wavelet analysis was performed with software based on tools provided by C. Torrence and G. P. Compo at <http://paos.colorado.edu/research/wavelets>.

Disclosure of Potential Conflicts of Interest

The authors declare that they have no conflicts of interest.

References

- Bárta, M., Karlický, M., Žemlička, R.: 2008, Plasmoid Dynamics in Flare Reconnection and the Frequency Drift of the Drifting Pulsating Structure. *Solar Phys.* **253**, 173. DOI. ADS.
- Bárta, M., Vršnak, B., Karlický, M.: 2008, Dynamics of plasmoids formed by the current sheet tearing. *Astron. Astrophys.* **477**, 649. DOI. ADS.
- Bárta, M., Karlický, M., Vršnak, B., Goossens, M.: 2007, MHD Waves and Shocks Generated during Magnetic Field Reconnection. *Central European Astrophysical Bulletin* **31**. ADS.
- Bárta, M., Büchner, J., Karlický, M., Skála, J.: 2011, Spontaneous Current-layer Fragmentation and Cascading Reconnection in Solar Flares. I. Model and Analysis. *Astrophys. J.* **737**, 24. DOI. ADS.
- Dabrowski, B.P., Karlický, M., Rudawy, P.: 2015, Fourier Analysis of Radio Bursts Observed with Very High Time Resolution. *Solar Phys.* **290**, 169. DOI. ADS.
- Farge, M.: 1992, Wavelet transforms and their applications to turbulence. *Annual Review of Fluid Mechanics* **24**, 395. DOI. ADS.
- Jelínek, P., Karlický, M., Van Doorselaere, T., Bárta, M.: 2017, Oscillations Excited by Plasmoids Formed During Magnetic Reconnection in a Vertical Gravitationally Stratified Current Sheet. *Astrophys. J.* **847**, 98. DOI. ADS.
- Jiříčka, K., Karlický, M.: 2008, Narrowband Pulsating Decimeter Structure Observed by the New Ondřejov Solar Radio Spectrograph. *Solar Phys.* **253**, 95. DOI. ADS.
- Karlický, M.: 2008, Separation of Accelerated Electrons and Positrons in the Relativistic Reconnection. *Astrophys. J.* **674**, 1211. DOI. ADS.
- Karlický, M.: 2013, Radio continua modulated by waves: Zebra patterns in solar and pulsar radio spectra? *Astron. Astrophys.* **552**, A90. DOI. ADS.
- Karlický, M.: 2014, Solar flares: radio and X-ray signatures of magnetic reconnection processes. *Research in Astronomy and Astrophysics* **14**, 753. DOI. ADS.
- Karlický, M., Bárta, M.: 2007, Drifting pulsating structures generated during tearing and coalescence processes in a flare current sheet. *Astron. Astrophys.* **464**, 735. DOI. ADS.
- Karlický, M., Bárta, M.: 2011, Successive Merging of Plasmoids and Fragmentation in a Flare Current Sheet and Their X-Ray and Radio Signatures. *Astrophys. J.* **733**, 107. DOI. ADS.
- Karlický, M., Kliem, B.: 2010, Reconnection of a Kinking Flux Rope Triggering the Ejection of a Microwave and Hard X-ray Source I. Observations and Interpretation. *Solar Phys.* **266**, 71. DOI. ADS.
- Karlický, M., Rybák, J.: 2017, Oscillation Maps in the Broadband Radio Spectrum of the 1 August 2010 Event. *Solar Phys.* **292**, 1. DOI. ADS.
- Karlický, M., Bárta, M., Rybák, J.: 2010, Radio spectra generated during coalescence processes of plasmoids in a flare current sheet. *Astron. Astrophys.* **514**, A28. DOI. ADS.
- Karlický, M., Mészáros, H., Jelínek, P.: 2013, Radio fiber bursts and fast magnetoacoustic wave trains. *Astron. Astrophys.* **550**, A1. DOI. ADS.
- Karlický, M., Rybák, J., Monstein, C.: 2017, Oscillations in the 45 - 5000 MHz Radio Spectrum of the 18 April 2014 Flare. *Solar Phys.* **292**, 94. DOI. ADS.
- Karlický, M., Bárta, M., Mészáros, H., Zlobec, P.: 2005, Time scales of the slowly drifting pulsating structure observed during the April 12, 2001 flare. *Astron. Astrophys.* **432**, 705. DOI. ADS.

- Kliem, B., Karlický, M., Benz, A.O.: 2000, Solar flare radio pulsations as a signature of dynamic magnetic reconnection. *Astron. Astrophys.* **360**, 715. ADS.
- Loureiro, N.F., Schekochihin, A.A., Cowley, S.C.: 2007, Instability of current sheets and formation of plasmoid chains. *Physics of Plasmas* **14**(10), 100703. DOI. ADS.
- Ohyama, M., Shibata, K.: 1998, X-Ray Plasma Ejection Associated with an Impulsive Flare on 1992 October 5: Physical Conditions of X-Ray Plasma Ejection. *Astrophys. J.* **499**, 934. DOI. ADS.
- Torrence, C., Compo, G.P.: 1998, A Practical Guide to Wavelet Analysis. *Bulletin of the American Meteorological Society* **79**, 61. DOI. ADS.

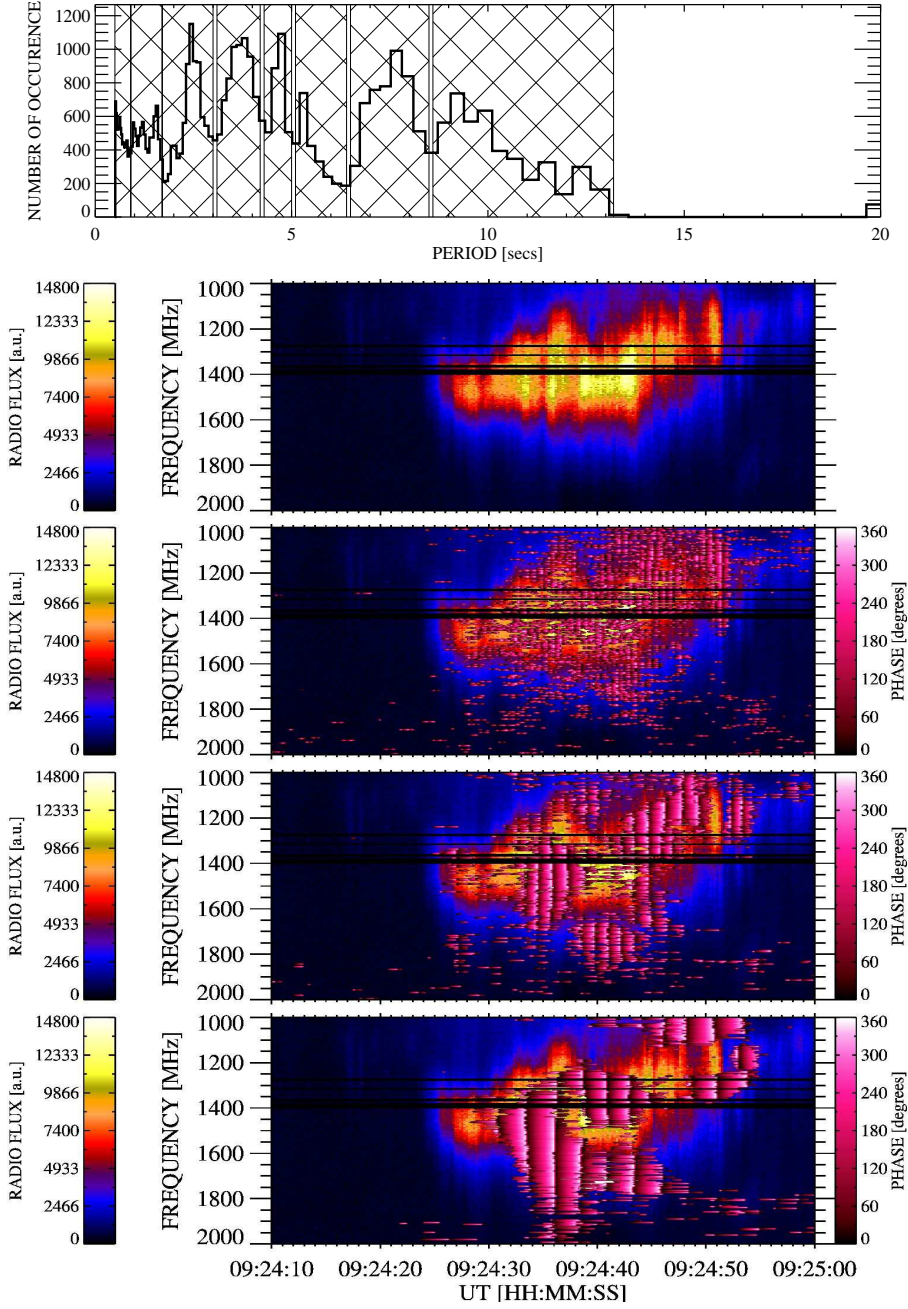


Figure 1. DPS in the 05 October 1992 flare — time interval 09:24:10–09:25:00 UT: *first panel* (from up to down): histogram of the WT significant periods, where the ranges of periods selected for the following oscillation maps are expressed by hatched areas; *second panel*: the radio spectrum observed by the *Ondřejov Radiospectrograph*; *bottom three panels*: the phase maps (pink areas with the black lines showing the zero phase of oscillations) overplotted on the radio spectrum for periods detected in the range of 0.5–0.9, 0.9–1.7, and 1.7–3.0 s.

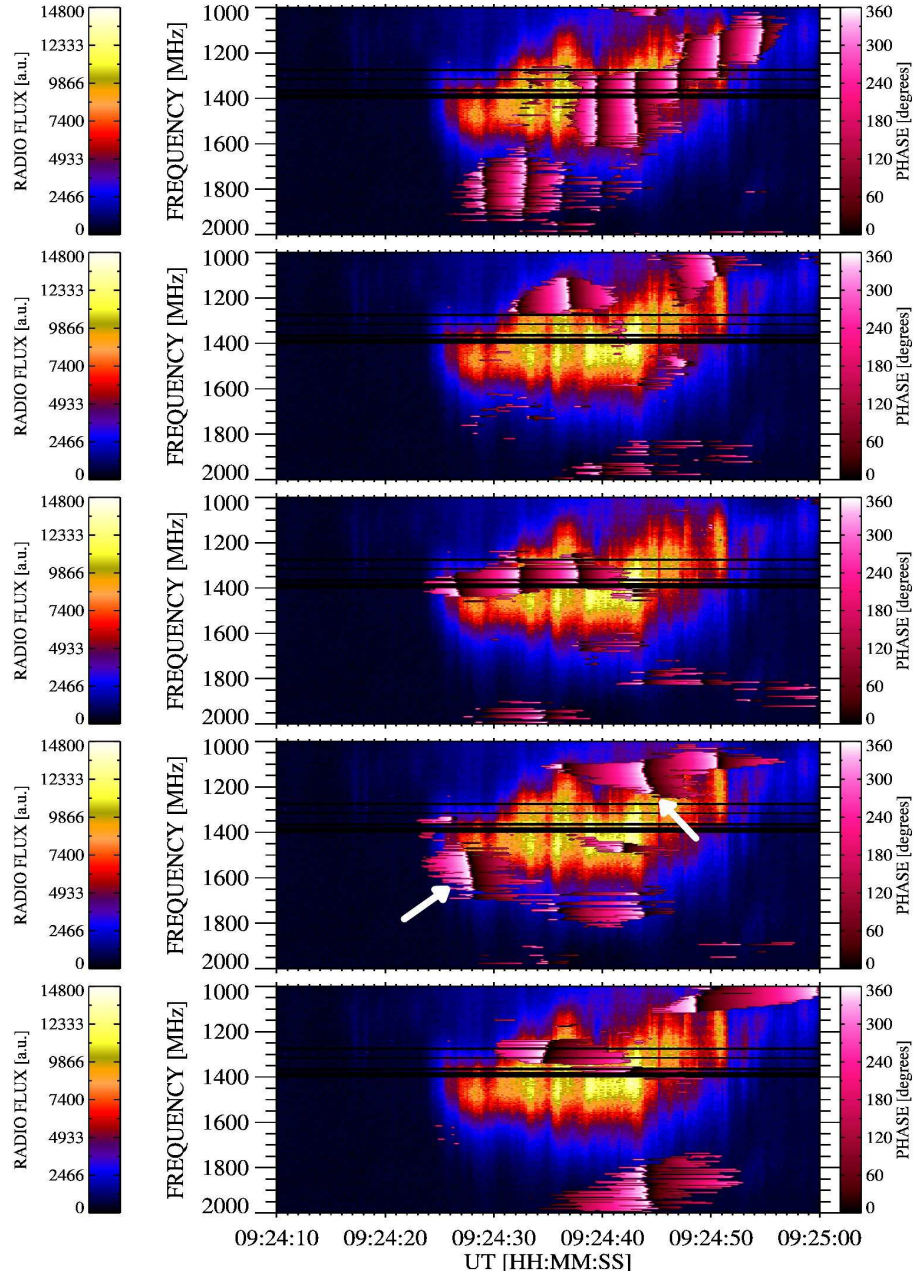


Figure 2. DPS in the 05 October 1992 flare — continuation of Figure 1 for longer periods: the phase maps (*pink areas with the black lines* showing the zero phase of oscillations) overplotted on the radio spectrum for periods detected in the range of 3.1–4.2, 4.3–5.0, 5.1–6.4, 6.5–8.5, and 8.6–13.2 s (*from up to down*). The *white arrows* show selected distinct drifting oscillation phases.

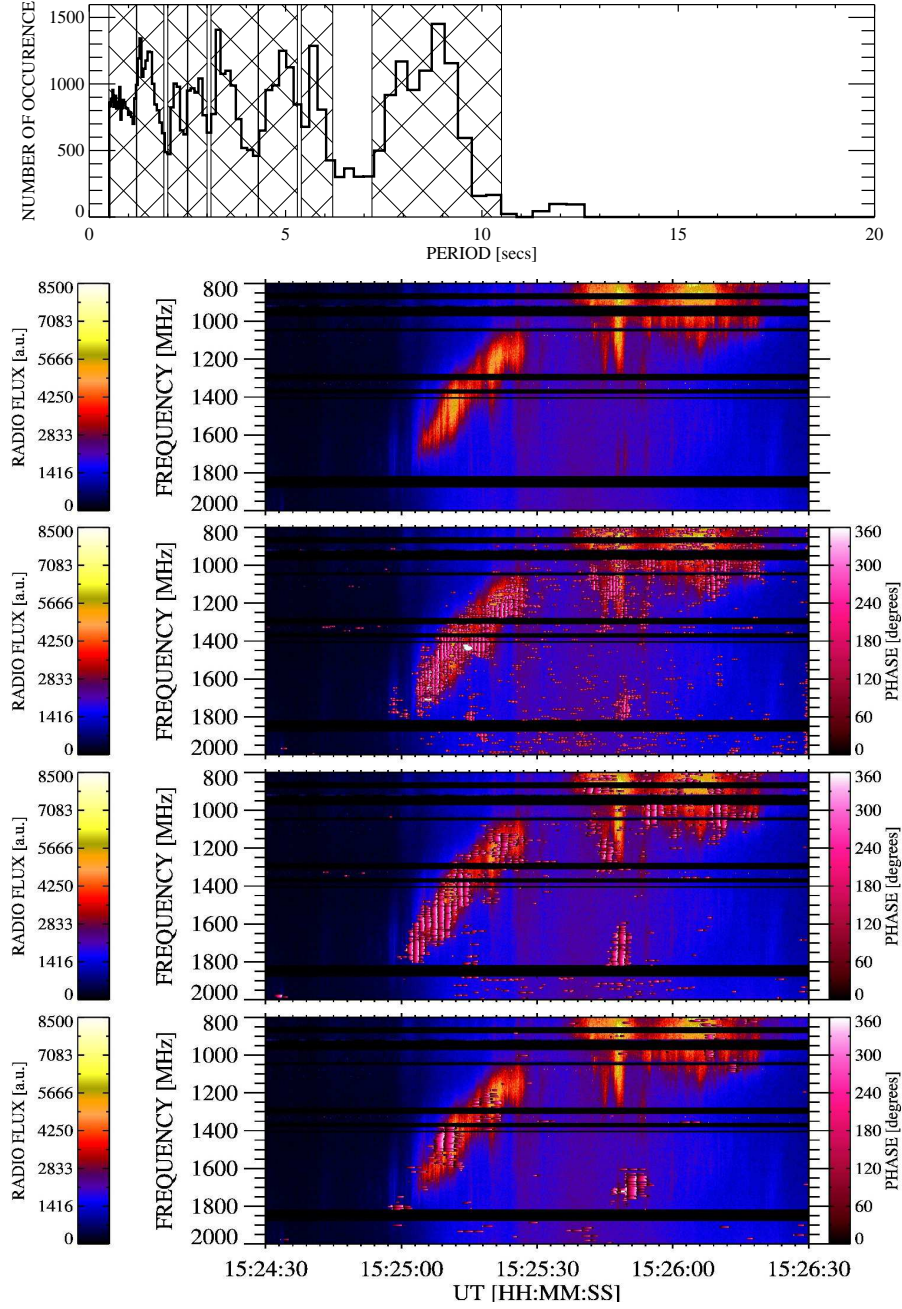


Figure 3. DPS in the 20 May 2002 flare — time interval 15:24:30–15:26:30 UT: *first panel* (from up to down): histogram of the WT significant periods, where the ranges of periods selected for the following oscillation maps are expressed by *hatched areas*; *second panel*: the radio spectrum observed by the *Ondřejov Radiospectrograph*; *bottom three panels*: the phase maps (*pink areas with the black lines* showing the zero phase of oscillations) overplotted on the radio spectrum for periods detected in the range of 0.5–1.2, 1.2–1.9, and 2.0–2.5 s.

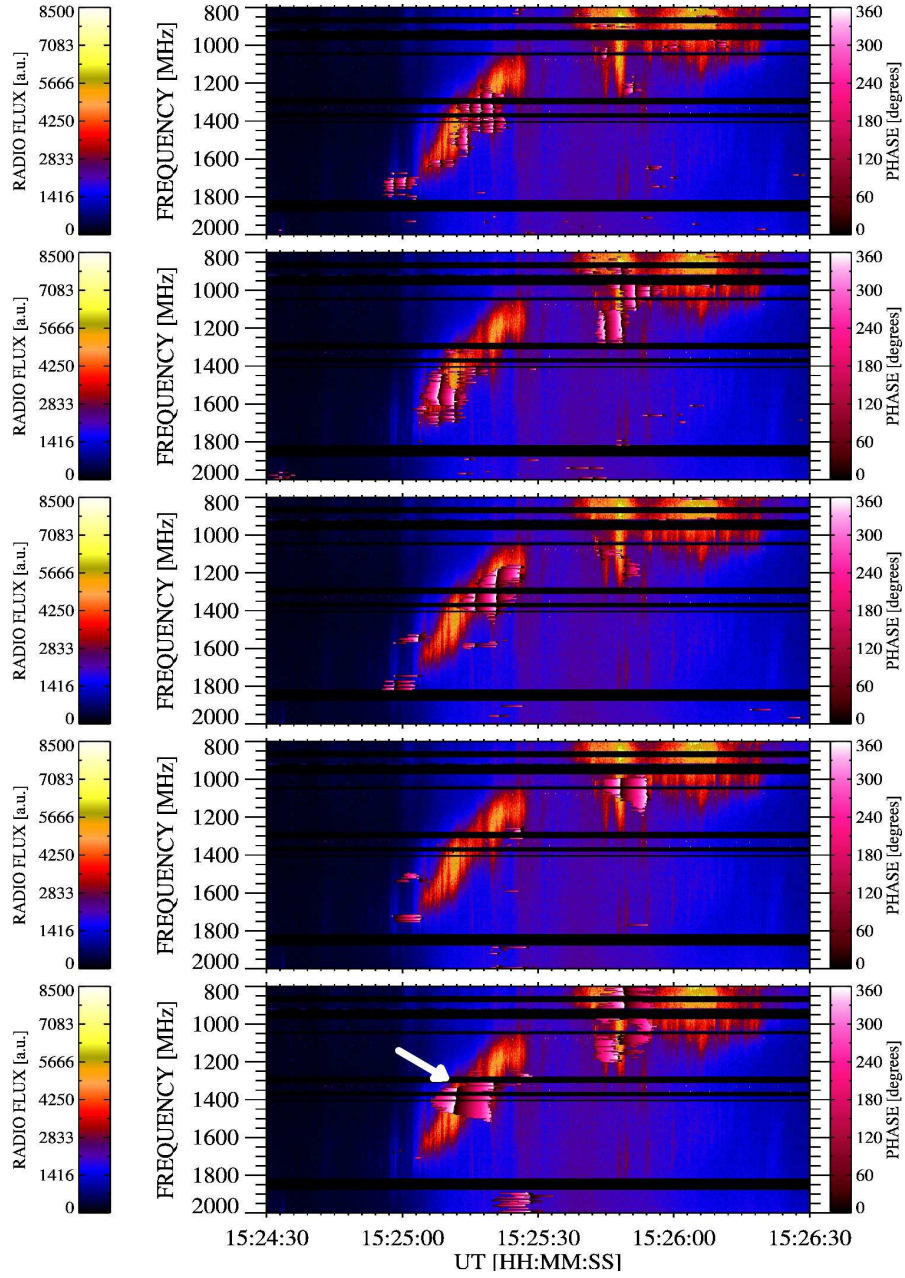


Figure 4. DPS in the 20 May 2002 flare — continuation of Figure 3 for longer periods: the phase maps (*pink areas with the black lines* showing the zero phase of oscillations) overplotted on the radio spectrum for periods detected in the range of 2.5–3.0, 3.1–4.3, 4.3–5.3, 5.4–6.2, and 7.2–10.5 s (*from up to down*). The *white arrow* shows selected distinct drifting oscillation phase.

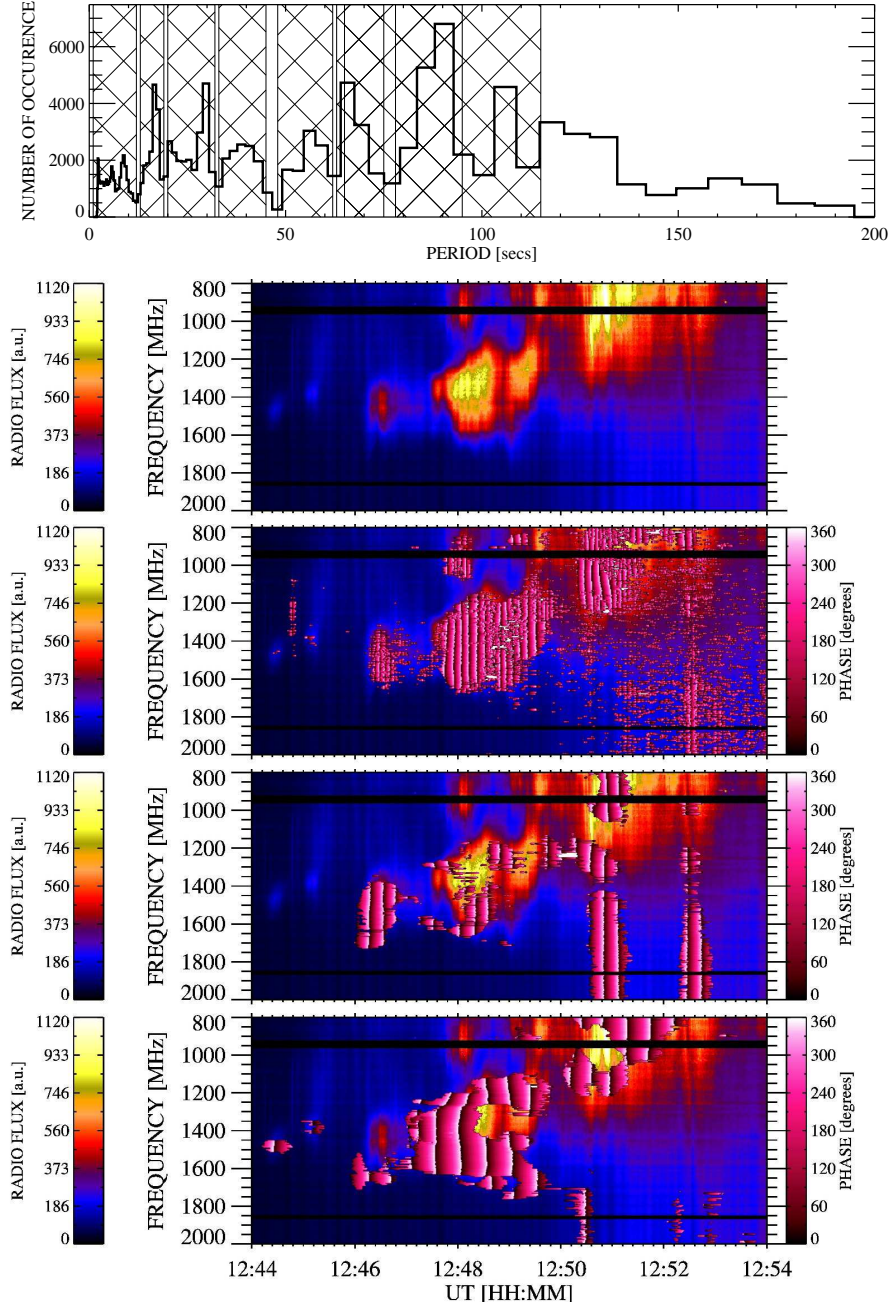


Figure 5. DPS in the 18 April 2014 flare — time interval 12:44:00–12:54:00 UT: *first panel* (from up to down): histogram of the WT significant periods, where the ranges of periods selected for the following oscillation maps are expressed by *hatched areas*; *second panel*: the radio spectrum observed by the *Ondřejov Radiospectrograph*; *bottom three panels*: the phase maps (*pink areas with the black lines* showing the zero phase of oscillations) overplotted on the radio spectrum for periods in the range of 1–12, 13–19, and 20–32 s.

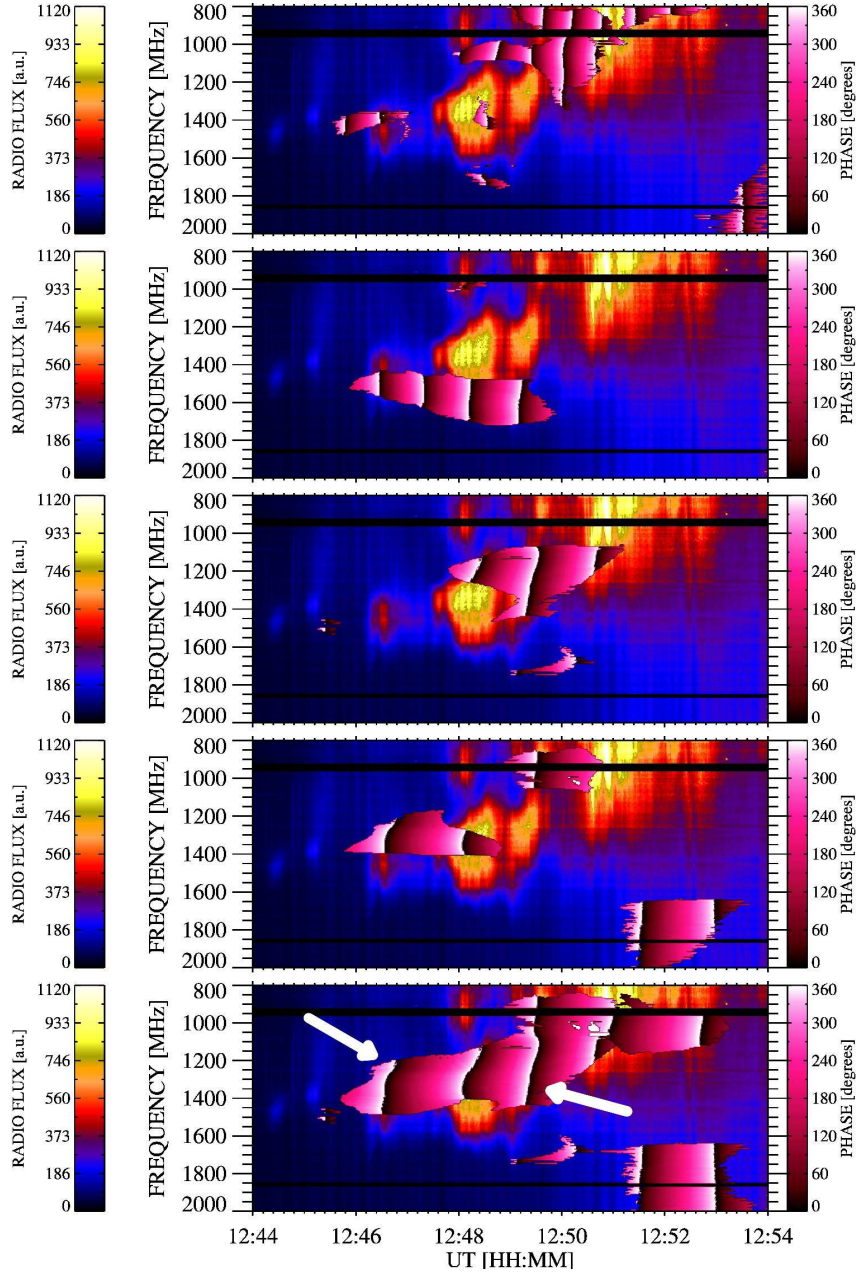


Figure 6. DPS in the 18 April 2014 flare — continuation of Figure 5 for longer periods: the phase maps (*pink areas with the black lines* showing the zero phase of oscillations) overplotted on the radio spectrum for periods detected in the range of 33–45, 48–62, 63–75, 78–95, and 65–115 s (*from up to down*). Note that the last interval of periods (65–115 s) covers the intervals of periods with 63–75 and 78–95 s. The *white arrows* show selected distinct drifting oscillation phases.